Atmos. Chem. Phys. Discuss., https://doi.org/10.5194/acp-2018-781
Manuscript under review for journal Atmos. Chem. Phys.
Discussion started: 30 August 2018

Atmospheric Chemistry and Physics Discussions

Core and margin in warm convective clouds. Part II: aerosol effects on core properties

[1]Reuven H. Heiblum, [1]Lital Pinto, [1]Orit Altaratz, [1]Guy Dagan, [1]Ilan Koren

[1]Department of Earth and Planetary Sciences, Weizmann Institute of Science, Rehovot, Israel

Corresponding Email – ilan.koren@weizmann.ac.il

Atmos. Chem. Phys. Discuss., https://doi.org/10.5194/acp-2018-781
Manuscript under review for journal Atmos. Chem. Phys.
Discussion started: 30 August 2018

Atmospheric Chemistry and Physics
Discussions

Abstract:

The effects of aerosol on warm convective cloud cores are evaluated using single cloud and cloud field simulations. As presented in Part I, the $B_{core} \subseteq RH_{core} \subseteq W_{core}$ property is seen during growth of warm convective clouds. We show that this property is kept irrespective of aerosol concentration. During dissipation core fractions generally decrease with less overlap between cores. However, for clouds that develop in low aerosol concentrations capable of producing precipitation, B_{core} and subsequently W_{core}volume fractions may increase during dissipation (i.e. loss of cloud mass). The RH_{core} volume fraction decreases during cloud lifetime and shows minor sensitivity to aerosol concentration.

It is shown that a B_{core} forms due to two processes: i) Convection – condensation within supersaturated updrafts and release of latent heat, ii) Adiabatic heating due to weak downdrafts. The former process occurs during cloud growth for all aerosol concentrations. The latter process only occurs for low aerosol concentrations during dissipation and precipitation stages where large mean drop sizes permit slow evaporation rates.

The aerosol effect on the diffusion efficiencies play a crucial role in the development of the cloud and its partition to core and margin. Using the RH_{core} definition, it is shown that the total cloud mass is mostly dictated by core processes, while the total cloud volume is mostly dictated by margin processes. Increase in aerosol concentration increases the core (mass and volume) due to enhanced condensation but also decreases the margin due to evaporation. In clean clouds larger droplets evaporate much slower, enabling preservation of cloud volume and even increase by dilution (detrainment while losing mass). This explains how despite having smaller cores and less mass, cleaner clouds may live longer and grow to larger sizes.

Atmos. Chem. Phys. Discuss., https://doi.org/10.5194/acp-2018-781
Manuscript under review for journal Atmos. Chem. Phys.
Discussion started: 30 August 2018

Atmospheric Chemistry and Physics Discussions
Open Access

1. Introduction

Aerosols remain one of the largest sources of uncertainty in climate predictions, mainly via their effects on clouds (IPCC, 2013). Here we focus on the aerosol effects on warm clouds. Aerosols act as cloud condensation nuclei (CCN) during heterogeneous nucleation by reducing the supersaturation required for droplet activation (Köhler, 1936;Mason and Chien, 1962), yielding differences in the initial cloud droplet size distribution (DSD). Polluted clouds have more, but smaller droplets, and a narrower DSD compared to clean clouds (Twomey, 1977;Andreae et al., 2004). Changes in the initial DSD drive various effects and feedbacks on the cloud's evolution and key processes, such as: droplet mobility, condensation/evaporation budgets, collision-coalescence, and entrainment (Jiang et al., 2006;Xue and Feingold, 2006;Small et al., 2009;Koren et al., 2015).

It is well known that an abundance of small droplets in a cloud (a narrow DSD) reduces the efficiency of the collision-coalescence process (Squires, 1958;Warner, 1968;Twomey, 1977), prolongs the diffusional growth time (Khain et al., 2005;Wang, 2005), and delays or even completely suppresses the initiation of precipitation (Hudson and Yum, 2001;Hudson and Mishra, 2007;L'Ecuyer et al., 2009;Albrecht, 1989). Moreover, in-cloud condensational growth is more efficient in consuming supersaturation because of the larger surface area-to-volume ratio of droplets (Mordy, 1959;Reutter et al., 2009;Pinsky et al., 2012;Seiki and Nakajima, 2013;Dagan et al., 2015a, b). These processes above enable the more polluted cloud to condense more water and intensify its growth via increased release of latent heat (Kogan and Martin, 1994;Koren et al., 2014). The smaller droplets are also pushed higher in the atmosphere due to larger droplet mobility (Koren et al., 2014;Koren et al., 2015)).

However, the increase in aerosol amount yields suppressing effects as well. The symmetry of the diffusion equation dictates that an opposite effect should take place in the sub saturated regions of the cloud, where more numerous and smaller droplets increase the evaporation rate and loss of cloud mass. Increased evaporation can promote entrainment mixing which in turn mixes more sub saturated air into the cloud and further promotes evaporation (Jiang et al., 2006;Xue and Feingold, 2006;Small et al., 2009), effectively initiating a positive feedback between evaporation and mixing with the eventual suppression of cloud growth. This effect may also be accompanied

Atmos. Chem. Phys. Discuss., https://doi.org/10.5194/acp-2018-781
Manuscript under review for journal Atmos. Chem. Phys.
Discussion started: 30 August 2018

Atmospheric Chemistry and Physics
Discussions

by a suppressing effect of the larger water loading in polluted clouds which contain more liquid water mass.

The competition between those opposing processes that are driven by enhanced aerosol loading determines the net aerosol effect on cloud properties such as cloud fraction, lifetime, albedo, mass, size, and precipitation amount. However, the sign and magnitude of such effects are non-trivial (Jiang and Feingold, 2006;Stevens and Feingold, 2009). Previous studies report opposing findings regarding the total aerosol effects on warm clouds (Altaratz et al., 2014). Some studies suggest cloud invigoration by aerosols (bigger and deeper clouds) (Kaufman et al., 2005;Dey et al., 2011;Yuan et al., 2011;Koren et al., 2014) while some suggest cloud suppression or no effect at all (Jiang and Feingold, 2006;Xue et al., 2008;Li et al., 2011;Savane et al., 2015). Moreover, other work has shown that the precipitation susceptibility (i.e. quantifies the sensitivity of precipitation to the aerosol increase) has a non-monotonic behavior that reaches its maximum at intermediate LWP values (Sorooshian et al., 2009), implying that the resultant aerosol effects are heavily dependent on cloud type and environmental conditions.

A unified theory for the contradicting results regarding aerosol effects was shown in recent work (Dagan et al., 2015b). It was shown that the competition between opposite processes leads to an optimum value of aerosol concentration regarding various cloud properties like total mass, cloud top, or rain. A cloud that develops under low aerosol concentration is aerosol limited, as it does not have enough collective droplet surface area to consume the available water vapor. On the other side of the trend, a cloud that develops in polluted environment (with more aerosols than the optimum) is influenced significantly by enhanced entrainment and larger water loading, causing suppression of cloud development. The optimal concentration is a function of the thermodynamic conditions (temperature and humidity profiles) and cloud size.

Environments that support larger clouds development will have larger cloud cores that are positively affected by aerosol increase and can be regarded as aerosol limited (i.e. on the ascending branch of the aerosol trend) up to a higher optimal aerosol concentration. Environmental conditions that support small clouds are more strongly affected by cloud suppression processes at the cloud margins (due to higher cloud surface area to volume ratio) and would have a lower optimal aerosol concentration. This can explain why studies biased to smaller clouds (mostly numerical modeling studies) report cloud suppression and studies biased to larger clouds (mostly observational studies) report cloud invigoration. Similar conclusions were reached for the cloud field scale as well (Dagan et al., 2017).

In addition, it was shown that clouds impact differently the environmental thermodynamics according to the aerosol level in the field (Seifert and Heus, 2013;Seifert et al., 2015;Dagan et al., 2016). For example changes in aerosol loading impact the amount of precipitation reaching the surface and subsequently the evaporative cooling below cloud base and the organization patterns (Xue et al., 2008;Seifert and Heus, 2013;Seigel, 2014). Moreover, an increase in aerosol loading may increase evaporation rates around the margins and tops of clouds (Xue and Feingold, 2006;Stevens, 2007;Seigel, 2014), cooling the upper cloudy layer and increasing the convective instability. Therefore aerosol effects on phase changes and precipitation result in vertical redistribution of heat and moisture, which may either stabilize or destabilize the environment in which subsequent clouds grow (Seifert and Heus, 2013).

Irrespective of the definition chosen, the cloud's core and margin are dominated by different processes (Dagan et al., 2015b). These processes often compete with each other, with the dominant one changing along the cloud’s evolution. For example, at the initial stage of cloud formation, a cloud is more adiabatic and is controlled by the core's processes (condensation), and when it dissipates the margin processes are more dominant (entrainment and evaporation). Aerosols affect each of these processes and thus each stage in the cloud’s lifetime.

2. Methods

The analyses performed here are to the most part identical to those described in Part I (hereafter PTI) of this work. In this section we shall thus only give a brief review of the methods used. For single cloud simulations we use the Tel-Aviv University axisymmetric cloud model (TAU-CM (Reisin et al., 1996)), and for cloud field simulations we use the System for Atmospheric Modeling (SAM) Model (version

Atmos. Chem. Phys. Discuss., https://doi.org/10.5194/acp-2018-781
Manuscript under review for journal Atmos. Chem. Phys.
Discussion started: 30 August 2018

6.10.3, for details see webpage: http://rossby.msrc.sunysb.edu/~marat/SAM.html) (Khairoutdinov and Randall, 2003)).

Both models utilize explicit bin microphysics schemes (Tzivion et al., 1987;Khain et al., 2004), solving nucleation, diffusion (i.e. condensation and evaporation), collisional coalescence, breakup, and sedimentation microphysical processes. The single cloud model is initialized using a Hawaiian thermodynamic profile, based on the 91285 PHTO Hilo radiosonde at 00Z, 21 Aug, 2007. The cloud field model is setup based on the BOMEX case study, including an initialization setup (sounding, surface fluxes, and surface roughness) and large scale forcing setup (Siebesma et al., 2003). More details on the model setups and definitions can be found in PTI.

To study the effects of aerosols on the cloud cores we run each model setup with three different aerosol concentrations: clean – 25 cm^{-3}, intermediate – 250 cm^{-3}, and polluted – 2000 cm^{-3}. As defined in Part I, all pixels with at least 0.01 g kg^{-1} of liquid water are considered cloudy. Cloud cores are defined using three definitions: 1) RH_{core}: relative humidity > 100%, 2) B_{core}: buoyancy > 0, and 3) W_{core}: vertical velocity > 0. Relative humidity (RH) and vertical velocity (W) are standard outputs of the model, while the buoyancy (B) is calculated based on eq. 1 in PTI, where each cloudy pixel is compared with the mean non-cloudy thermodynamic reference state per height.

In order to reduce the problem’s dimensionality and distill signals in a cloud field system governed by high variance, we use the Gravity vs. Mass (CvM) phase space in combination with an automated 3D cloud tracking algorithm (Heiblum et al., 2016b). The CvM phase space enables a compact view of all clouds in the simulation, by projecting only their Center-of-Gravity (COG) height and mass at each output time step. Using the cloud tracking, it was shown that the lifetime of a cloud can be described by a trajectory on this phase space. Hence, the different locations in the CvM space are associated with different stages in a cloud's lifetime (i.e. growing, precipitating, and dissipating). For an in-depth explanation of the CvM space, the reader is referred to Sect. 2.4 in PTI (see schematic illustration - Fig. 1, PTI).

3. Results – Single cloud simulations

3.1. Sensitivity of different core types to aerosol concentration

Figure 1 presents time series of single cloud core volume fractions and cores' properties, for three aerosol concentrations (clean, intermediate, and polluted). Also included are time series of instantaneous rain-rates [mm hr^{-1}] at the domain surface. For all aerosol concentrations and during most of the clouds' lifetimes, the volume fraction of W_{core} tends to be the largest and of B_{core} the smallest. Exceptions to this finding are seen either at the initial time step for the polluted cloud or the later stages of cloud lifetime for the lower concentration clouds. In addition, we find that $RH_{core} \subseteq W_{core}$ for all stages of cloud lifetime while $B_{core} \subseteq W_{core}, RH_{core}$ for all stages of the polluted cloud but only applies to the growing stages of lower concentration clouds before precipitation production. Thus, the main finding from PTI (i.e. $B_{core} \subseteq RH_{core} \subseteq W_{core}$) generally applies to all aerosol concentrations during the pre-precipitation stages of the clouds' lifetimes.

Lower aerosol concentration simulations produce more rain, and at earlier stages of cloud lifetime due to efficient collision coalescence. The increase in B_{core} volume fraction at later stages of cloud lifetime in those simulations (clean and intermediate) coincides with initiation of precipitation production, followed by a consequent increase in W_{core} volume fraction as well (more so for the intermediate concentration). The possible mechanism behind the increase in prevalence of buoyant parcels during precipitation is explored in Sect. 3.2. The lack of RH_{core} pixels at these stages indicates that the W_{core} is composed of pixels with small vertical velocities, insufficient for supersaturation production. The RH_{core} is the only one which is not sensitive to rain and monotonically decreases during all clouds' lifetimes. Another clear aerosol effect seen in Fig. 1 is an increase in cloud lifetime with decrease in aerosol concentration. This point will be further explored in Sect. 3.3.

3.2. Mechanisms governing positive buoyancy

The theoretical arguments in PTI showed that B_{core} should be the smallest of the three. This was shown for both the adiabatic cloud column case and also the non-adiabatic case where entrainment mixing and consequent evaporation has a strong net

Atmos. Chem. Phys. Discuss., https://doi.org/10.5194/acp-2018-781
Manuscript under review for journal Atmos. Chem. Phys.
Discussion started: 30 August 2018

negative effect has on cloud buoyancy. Despite this fact, results show (see Fig. 1, and Fig. 2 in PTI) that pockets of positive buoyancy may form independent of the other cores during dissipation and precipitation stages, even though evaporation is to be expected then. Since positive buoyancy is the result of either higher temperature or vapor content (or both) than the surrounding environment, we choose to analyze these two terms during different stages of the single cloud lifetimes.

Figure 2 shows the values of the temperature (B_T) and humidity (B_{Qv}) buoyancy terms in pixel buoyancy vs. pixel vertical velocity phase space. The scatter plots include all cloudy pixels during all time steps, for the three different aerosol concentration simulations. The distribution of points for the polluted simulation shows a positive linear dependence of buoyancy on vertical velocity. Negative vertical velocity is associated with negative buoyancy and positive vertical velocity shows a transition from negative to positive buoyancy with increase in magnitude. For this case both B_T and B_{Qv} increase with increase in vertical velocity, as is generally expected in convective clouds. The sign of pixel buoyancy is mostly dependent on B_T since all pixels have positive B_{Qv} and a negative water loading term. This behavior is also seen for lower aerosol concentrations, where the sign of buoyancy is to the most part determined by $B_{T.}$

The clean and intermediate simulations show a similar dependence of buoyancy on vertical velocity; however, it is apparent that these simulations also include an outlier scatter region of pixels with positive buoyancy and weak negative vertical velocity which is absent in the polluted simulation (see white arrows, Fig. 2). Consistent with the rest of the cloudy pixels, these outlier pixels have positive B_T, but differ in that they show neutral B_{Qv}. It can also be seen that these pixels are only attributed to the stages after surface precipitation has commenced (indicated by black dots in markers). Precipitation is indicative of both downdraft motion and abundance of large droplet sizes.

Thus, we hypothesize that pockets of positive buoyancy may form due to transport of parcels with higher potential temperature from above, namely adiabatic heating. The weak downdrafts also transport lower mixing ratio (Q_v) values, as is indicated by the neutral B_{Qv}. Moreover, the occurrence during precipitating stages and for lower aerosol concentrations indicates that slow evaporation due to larger droplet sizes is

Atmos. Chem. Phys. Discuss., https://doi.org/10.5194/acp-2018-781
Manuscript under review for journal Atmos. Chem. Phys.
Discussion started: 30 August 2018

crucial. Indeed, most pixels with negative buoyancy show positive B_{Qv} except for the clean case where rain pixels from the cloudy layer sediment well below the cloud base and experience higher environmental Qv (while evaporating slowly), resulting in negative B_{Qv}.

3.3. The dependency of cloud characteristics on core and margin's processes

Here we evaluate how aerosol effects within the core and margin affect the cloud characteristics, focusing on two main parameters; size (or volume) and mass. In Fig. 3 we follow the evolution of cloud, core, and margin mass and volume for different aerosol concentrations, using only the RH_{core} definition. We choose the RH_{core} since it is the most well behaved out the core types, generally decreasing monotonically (see Fig. 1). A non-monotonic dependency of total cloud mass on aerosol concentration is seen, showing a maximum for the intermediate concentration. This type of dependency has been previously reported for warm cumulus clouds (Dagan et al., 2015b;Savane et al., 2015).

One can generally expect an increase in diffusion and decrease in collision-coalescence processes efficiency with increase in aerosol concentration (Hudson and Yum, 2001;Jiang et al., 2009;L'Ecuyer et al., 2009;Pinsky et al., 2012), affecting both condensation and evaporation processes. The intermediate concentration shows the highest total mass as a result of being an optimal case with higher condensation efficiency than the clean case and lower evaporation efficiency than the polluted case. It is convenient to represent the condensation and evaporation efficiencies by the RH_{core} and RH_{margin} mass, respectively. The intermediate cloud has almost identical core mass as does the polluted cloud, but retains higher mass in its margin as well. The clean cloud shows the lowest core mass but manages to accumulate the largest mass in its margin that dissipates slowly in subsaturated conditions. By comparing the total cloud mass evolution with the core and margin mass evolutions, it becomes clear that the total mass is primarily dependent on the cloud core. Another way to see this is by plotting the core mass fraction (Fig. 3 bottom panel), which shows that clouds are core dominated (core fraction > 0.5) with respect to mass for most of their lifetimes, and for all aerosol concentrations.

With respect to cloud total volume, the lower the concentration, the larger the total cloud volume. We note that the cloud volume here excludes regions of precipitation below the initial cloud base height. By separating to core and margin regions, one can see that the total cloud volume is primarily dependent on the volume of the margin, which increases significantly with decreasing concentration. This is especially true during the dissipating stages of cloud lifetime, when the cloud is margin dominated. Although increasing the aerosol concentration does initially yield an increase in core volume (as was seen for the mass), the extents of the core size are typically smaller than those of the margin. There are large differences in the relative core volume percent for the different clouds. The clean (polluted) cloud is margin (core) dominated with respect to volume for most of its lifetime. Excluding time of formation, the clean cloud shows the lowest core volume fractions, but manages to maintain its core for the longest time span.

These results can again be attributed to higher diffusion efficiencies with increase in aerosol concentration. Additionally, lower collision-coalescence efficiencies also maintain a narrow droplet spectrum of small droplets in the polluted cloud. During the growing stage a higher aerosol concentration may permit the cloud to condense more water, release more latent heat, and promote cloud growth. This explains the larger core volume sizes. However, after the cloud exhausts its convective potential (i.e. the growth of the convective core terminates and reaches its peak in mass), its main method of expansion is by mixing with the environment (i.e. detrainment). We note that precipitation can also be considered a method of expansion, however our choice to focus on volume above initial cloud base excludes this effect. Detrainment results in sub-saturation conditions and evaporation of LWC. A clear indication for dilution is seen in Fig. 3 where between 30 and 35 mins of simulation time both the clean and polluted clouds lose total mass but only the clean cloud increases in total volume. The polluted cloud evaporates its margin regions efficiently and is thus limited in detrainment growth. The clean cloud is less efficient in evaporating its margins and hence can grow by dilution of its LWC upon a larger volume. This large margin "shields" the core during dissipation stages and enables it the live for a longer time.

The mechanism behind the results in Fig. 3 is demonstrated in Fig. 4, where horizontal cross-sections of mean (taken in the vertical dimension) cloud RH are shown for different stages during the clouds' lifetimes. For the polluted cloud, super-

Atmos. Chem. Phys. Discuss., https://doi.org/10.5194/acp-2018-781
Manuscript under review for journal Atmos. Chem. Phys.
Discussion started: 30 August 2018

or sub- saturated conditions are rare. The RH throughout the cloud is near 100% (almost always between 99.8% and 100.2%) except for a few pixels at its far edges which are a bit below 99%. The polluted cloud resembles what one would expect to see using a moist adiabatic approximation (i.e. saturation adjustment), where all excess water vapor above saturation is converted to liquid water, mimicking infinitely efficient condensation (and evaporation).

The clean cloud shows opposite behavior, with extremes of large super-saturation during cloud growth (initial stages) and large sub-saturation during cloud dissipation (final stages). Both extremes can be explained by the low diffusion efficiency in this case**.** This enables the clean cloud to expand to larger horizontal extents (by dilution and mixing with the environment without fully evaporating) and live for longer times. The intermediate aerosol concentration shows a midway scenario, where the super-saturation is consumed more efficiently than the clean case and at the same time much larger values of sub-saturation may exist than those seen for the polluted case.

4. Results – Cloud field simulations

In the following section we expand our analyses of aerosol effects on cloud core and margin from the single cloud scale to the cloud field scale. A cloud field can be considered as composed of many individual clouds and thus can serve to test the robustness of the aerosol effects seen for a single cloud. Moreover, cloud fields include the added complexity of interactions between clouds and the clouds' effects on their thermodynamic environment.

4.1. Sensitivity of different core types to aerosol concentration

Here CvM space representations (see Sect. 2) are used to observe the core volume fractions of all clouds in BOMEX cloud field simulations. The rows in Fig. 5 represent different aerosol concentrations while the columns represent different core type definitions. Different aerosol concentrations produce a vastly different scatter of clouds in the CvM space, as was previously discussed in depth (Heiblum et al., 2016a). The clean simulation (25 cm^{-3}) shows two disconnected regions of cloud scatter: one which is adjacent to the adiabatic approximation and one of mainly small mass and high COG clouds. The former region includes both clouds during their growth stages (smaller masses, LWP < 10 g m^{-2}) and large precipitating entities (larger masses, LWP > 10 g m^{-2}) which form due to merging processes (see (Heiblum et al., 2016a)). The latter region (small mass and high COG) includes clouds at their dissipating stage, which form by shedding mechanism off the large cloud entities. We note also the existence of small mass elements well below the adiabat, representing precipitation cloud segments which shed off large precipitating clouds.

The polluted simulation (2000 cm^{-3}) shows a much more homogeneous scatter of clouds. The lower part of the scatter (closest to the adiabat) represents the cloud growing branch while the rest of the scatter represents dissipating clouds, either by gradual process of rising cloud base or by immediate process of shedding off larger cloud entity (see Fig. 1, PTI). Precipitating cloud segments below the adiabat are absent from this simulation. The intermediate simulation (250 cm^{-3}) shows a scatter which generally more resembles the polluted case. However, the existence of relatively disconnected (from the main cloud scatter) small mass cloud segments below the adiabat and near the inversion base height resembles the clean simulation as well.

The results in Fig. 5 show a consistent behavior of the core volume fractions for all aerosol concentrations, where the W_{core} type shows the largest fractions and the B_{core} type shows the smallest fractions. The W_{core} and RH_{core} generally show a decrease in core fractions along the growing branch while the B_{core} fraction initially increase with cloud growth and then decrease for the large mass growing clouds. These results are consistent with PTI and the single cloud simulations in Sect. 3.1. Nevertheless, some significant aerosol effects on the partition to core types can be seen. Focusing on the growing branch first (i.e. clouds located near the adiabat), we note the following:

1) For the RH_{core} type, the core volume fractions of clouds after formation (i.e. with small mass) increase with decreasing aerosol concentration. This effect was also seen for the single cloud simulations and can be explained by the reduced efficiency of super-saturation consumption for fewer aerosols.

2) The B_{core} volume fraction increases at smaller mass values (or earlier in cloud's lifetime) and to higher values for increasing aerosol concentration. This effect is complimentary to the previous one, since efficient consumption

Atmos. Chem. Phys. Discuss., https://doi.org/10.5194/acp-2018-781
Manuscript under review for journal Atmos. Chem. Phys.
Discussion started: 30 August 2018

of super-saturation should result in more latent heat release and positive buoyancy.

3) The core volume fractions of the largest mass clouds increase with increasing aerosol concentration, for all core types.

For the dissipating branch clouds a highly variable pattern of core volume fractions can be seen, especially for the small mass clouds. For all aerosol concentrations, these small cloud fragments can be either core dominated, margin dominated, or equally partitioned. One can assume that these differences can be related to the different mechanisms by which cloud fragments form, either by gradual dissipation of a large cloud and by instantaneous shedding of a large cloud. As for aerosol effects on the dissipating clouds, we see the following:

1) Higher RH_{core} and W_{core} volume fractions for gradually dissipating clouds (by rising cloud base) with increase in aerosol concentration. This is manifested by a slower transition from red to blue colors in Fig. 5. It can be explained by the fact that more aerosols increase the convective intensity and extend the core size, while efficiently losing the margins, yielding a higher core volume fraction out of the total cloud.

2) The likelihood to find dissipating cloud fragments with a B_{core} increases with decrease in aerosol concentration. For the polluted case most of the dissipating clouds lack a B_{core}. This effect was seen in Fig. 1 and explained in Sect. 3.2, showing that weak downdrafts promote heating and positive buoyancy in low aerosol concentration cases where evaporation efficiency (and hence cooling) is limited. This hypothesis is checked for the cloud field scale in Sect. 4.2.

As opposed to the single cloud simulations (Sect. 3) where cloud lifetime can be easily defined, in cloud field simulations (especially the cleaner cases) many clouds do not live as individual clouds from formation to dissipation but rather split and merge with other clouds continuously (Heiblum et al., 2016a). Thus, in order to evaluate the lifetime evolution of cores in cloud fields, we focus on the growing branch and use cloud mass [kg] as a proxy for the cloud lifetime during its initial and mature stages. We assume that in the vicinity of the growing branch a larger mass corresponds to a later stage in lifetime.

Atmos. Chem. Phys. Discuss., https://doi.org/10.5194/acp-2018-781
Manuscript under review for journal Atmos. Chem. Phys.
Discussion started: 30 August 2018

In Fig. 6 the core mass and volume fractions (using the RH definition) of all growing branch clouds are sorted by mass for the three aerosol concentrations. We note that the higher cloud masses reached by lower aerosol concentration simulation can be explained by cloud field organization effects due to precipitation (i.e. increased merging of clouds) rather than increased cloud condensation (Seigel, 2014;Heiblum et al., 2016a). The clean case starts off with the highest core fractions (both mass and volume) which decrease steadily with increase in mass (or increase in lifetime). For all concentrations, most of the cloud mass is concentrated in the core region. The polluted case shows a slight increase in mass fractions with increase in mass, while the other two cases show decreases in mass fractions.

The core volume fractions show lower values than the mass fractions. The clean clouds are margin dominated for most masses, and the polluted clouds are core dominated for all masses. The intermediate case is generally confined to values between the other two cases. Figure 6 can be considered comparable with the lower panels in Fig. 3, but excluding the dissipating part of those time series. The similar findings in both figures indicate the robustness of the aerosol effects on core properties in clouds.

Following the analyses of Sect. 3.1, we next test how aerosol concentration affects the subset properties of one core type within another for all clouds in a field (Fig. 7). We focus only on the typically smaller sized cores (B_{core}, RH_{core}) within larger sized cores. Out of the three permutations, the RH_{core} inside W_{core} shows the lowest sensitivity to aerosol. All three growing branches (for the different aerosol concentrations) consistently show that the RH_{core} is a subset of W_{core} (i.e. $RH_{core} \subseteq W_{core}$) while the dissipation branches show much lower overlap fraction between the two cores.

Generally, for the dissipating clouds, the lower the mass and the higher the COG, the smaller the overlap. The dissipating branches do include a scatter of small cloud for which $RH_{core} \subseteq W_{core}$, comprised of small cloud segments which shed of the main core regions of larger clouds. These findings slightly differ from those of the single cloud simulations that show $RH_{core} \subseteq W_{core}$ for their entire lifetimes while for cloud fields this property breaks downs during dissipation. This difference highlights the importance of cloud interactions (i.e. splitting, merging) and cloud field air flow

Atmos. Chem. Phys. Discuss., https://doi.org/10.5194/acp-2018-781
Manuscript under review for journal Atmos. Chem. Phys.
Discussion started: 30 August 2018

patterns (i.e. organized advection, updrafts, and downdrafts) in determining the relationships between core types, enabling supersaturation and downdrafts to coincide in small dissipating clouds.

The other two permutations (i.e. B_{core} inside RH_{core}, W_{core}) show significant changes due to aerosol. For the polluted case, $B_{core} \subseteq W_{core}$ for nearly all clouds, including clouds at initial stages of dissipation. Similar results are seen for B_{core} inside RH_{core}, but with slightly lower pixel fractions. The polluted case thus illustrates the case of buoyancy production due to convective processes. For the lower aerosol concentrations, two main aerosol effects are seen:

1) The lower the concentration, the lower the chance that B_{core} is a proper subset of the other cores for large growing branch clouds.

2) The lower the concentration, the more prevalent the independent dissipating branch B_{core} that has little to no overlap with the other cores.

For the case of B_{core} within RH_{core}, the lower concentrations show an almost binary scenario where either $B_{core} \subseteq RH_{core}$ or $B_{core} \notin RH_{core}$. These result bear similarity with the single cloud simulations, where a quick transition (in time) from $B_{core} \subseteq RH_{core}$ to $B_{core} \notin RH_{core}$ was seen. This results implies the existence of two different buoyancy production processes (as will be shown in Sect. 4.2), one associated with supersaturation and the other with subsaturation. In contrary, B_{core} inside W_{core}, which shows higher values and more fluctuations in pixels fractions for both single clouds and clouds fields during dissipation. This is to be expected due to the a more direct physical link and feedbacks between the B_{core} and W_{core}.

4.2. Analysis of cloud field buoyancy

In Sect. 3.2 it was seen that for single clouds, positive buoyancy results from two main mechanisms: i) convection - where updrafts promote supersaturation and latent heat release, and thus positive B_T and B_{Qv}, and ii) adiabatic heating – where weak downdrafts promote a positive B_T and neutral B_{Qv}. The latter case is dependent on low evaporation efficiency and hence seen mostly for precipitating stages of low aerosol concentration simulations.

Atmos. Chem. Phys. Discuss., https://doi.org/10.5194/acp-2018-781
Manuscript under review for journal Atmos. Chem. Phys.
Discussion started: 30 August 2018

Atmospheric Chemistry and Physics
Open Access
Discussions

In Fig. 8 we perform a similar test for the cloud field scale. Instead of analyzing pixel by pixel, we check whether each buoyancy core within a cloud is B_T or B_{Qv} dominated. To quantify this we use a normalized buoyancy dominance parameter $\frac{\Sigma pixel_{B_{T>0}} - \Sigma pixel_{B_{Qv>0}}}{\Sigma pixel_{B>0}}$, where a core comprised of only $B_T>0$ ($B_{Qv}>0$) pixels yields 1 (-1). Hence, we expect negative (positive) values to indicate dominance of convective buoyancy (adiabatic heating buoyancy).

Analysis of the buoyancy components in the CvM space (right column, Fig. 8) shows that the large majority of clouds are B_{Qv} dominated. For all concentrations, clouds initiate with all pixels showing $B_{Qv}>0$.As clouds develop along the growing branch the B_{core} becomes more abundant with $B_T>0$ pixels. This is expected with increasing release of latent heat during cloud growth. During dissipation B_{Qv} again becomes the dominant component for the majority of clouds. The polluted simulation shows an extreme case where all buoyancy cores in the simulation are B_{Qv} dominated, while for the lower concentrations a portion of the dissipating and precipitating clouds are B_T dominated.

Thus, we hypothesize that the polluted simulation only permits buoyancy cores of the convective type which intersect with the other cores types (i.e. $B_{core} \in RH_{core}, W_{core}$), while the lower concentrations also permit buoyancy cores of the adiabatic heating type which do not intersect with the other core types (i.e. $B_{core} \notin RH_{core}, W_{core}$). This hypothesis is tested by observing the effects of cloud maximum vertical velocity (left column, Fig. 8) and mean drop size (middle column, Fig. 8) on the relative dominance of the buoyancy terms. The data is further separated to independent ($B_{core} \notin RH_{core}, W_{core}$) and dependent ($B_{core} \in RH_{core}, W_{core}$) buoyancy subsets of the data. Clear aerosol effects are seen on cloud mean drop size and maximal W. As expected, there is a decrease in drop size with increase in aerosol concentration and increase in maximal velocity. Regarding cloud field buoyancy, as predicted the independent buoyancy cores are more frequently B_T dominated than the dependent buoyancy cores.

The polluted case is populated with dependent cores (white scatter) and shows a classic pre-precipitation convective growth scenario, where relative dominance of the B_T term increases linearly with increase in cloud mean drop size. A logarithmic dependence of B_T dominance on maximal W is seen, which saturates at high maximal

Atmos. Chem. Phys. Discuss., https://doi.org/10.5194/acp-2018-781
Manuscript under review for journal Atmos. Chem. Phys.
Discussion started: 30 August 2018

Atmospheric Chemistry and Physics Discussions

W. This can be explained by the fact increased convection mainly increases the abundance of pixels with $B_T > 0$, but without changing the fact that the entire cloud is $B_{Qv} > 0$, so that B_T is unlikely to become the dominant term.

The lower concentrations show a more complex scenario. These simulations show a superposition of dependent core convective growth behavior (i.e. the scatter pattern seen for the polluted case) and additional populations of both dependent (other white scatter points) and independent (black scatter) cores. The independent cores span all the range of possibilities of B_T and B_{Qv} relative dominances. They tend to have larger cloud mean drop sizes, and near zero maximum W, indicating that they only form at late non-convective stages of cloud development. The independent cores that are $B_T$dominated thus fulfill the characteristics of adiabatic heating process, while the independent cores that are B_{Qv} dominated may originate from larger clouds (shedding mechanism) with high humidity content and are slow to evaporate.

The intermediate simulation shows an additional scatter area of dependent core clouds with increasing of B_T relative dominance for lower maximal W, located between the independent core clouds and the convective growth core clouds. These clouds may represent a gradual transition fromB_{Qv} dominance to B_T dominance during dissipation which is only possible in the intermediate simulation. This scatter area is absent from the clean and polluted simulation. In the former case due to absence of the gradual dissipation pathway, and in the latter case due to efficient evaporation eliminating B_{core} during dissipation.

4.3. Aerosol effects on cloud relative humidity

From Fig. 3 it was learned that a large part of the differences in single cloud characteristics (such as mass, volume, and the partition of these to core and margin regions) due to aerosols can be attributed to differences in vapor diffusion efficiencies. In Fig. 9 we check how these aerosol effects are manifested in the cloud field scale (using the CvM space) by observing the mean relative humidity (RH) in the cloud core and margin of all clouds. The core mean RH can be taken as a proxy for condensation efficiency, the margin mean RH as a proxy for evaporation efficiency. To gain additional intuition regarding the distribution of RH values within the clouds, vertical cross-sections (parallel to the prevailing wind direction) of the most massive clouds from each simulation are shown.

The vertical cross-sections demonstrate the large differences in the massive clouds for each of the simulations. In addition to the increase in precipitation production, lower aerosol concentrations yield much larger horizontal extents of clouds. The clean, intermediate, and polluted most massive clouds have a maximum radius of ~ 3, ~ 1, and ~ 0.5 km, respectively. It is clear from the cross-section that the clean cloud is actually composed of two large clouds which merge together. For the clean case, the highest RH values are reached slightly below the cloud top. The edges of the clouds show sub-saturation conditions, with the lowest RH values observed below the LCL (precipitation regions) and at the upper interface of the cloud with the environments.

The intermediate case cloud shows lower maximal and minimal RH values and an increased dominance of the margin region. This cloud penetrates the inversion layer and entrains dry air into the cloud. In addition, the cloud produces significant precipitation which initiates downdrafts of dry entrained air through the cloud center. It can be seen that the increased vertical development of the intermediate case cloud in comparison with the clean case increases the mixing with the environment. Thus, the dynamic effect of increased mixing and reduction in cloud RH overcomes the microphysical effect of increased evaporation and increase in cloud RH. The polluted case cloud on the other hand shows a homogeneous RH pattern, with most of the cloud showing around 100% RH and only a thin layer at the cloud edges (mainly at the upper regions) shows lower RH values. The polluted cloud penetrates the inversion layer as well, but this case lacks precipitation and the microphysical effect of evaporation overcomes the dynamical effect of mixing.

Keeping in mind the insights obtained from comparisons of individual cloud, we move on to compare the RH characteristics of all clouds within the field. Looking first at core mean RH, a robust decrease is seen with increase in aerosol concentration. This decrease is seen for all cloud types and locations within the CvM space. The polluted case displays the most homogeneous pattern with all clouds showing core mean RH values around 100%, indicating efficient consumption of the supersaturation. The intermediate case displays a slightly less homogeneous pattern with values ranging from 100% to 101%, the higher values occurring along the

Atmos. Chem. Phys. Discuss., https://doi.org/10.5194/acp-2018-781
Manuscript under review for journal Atmos. Chem. Phys.
Discussion started: 30 August 2018

Atmospheric Chemistry and Physics
Discussions

growing cloud branch, especially for the largest clouds. The clean case shows the largest variance in core mean RH, ranging from 100% for some cloud fragments that soon start to dissipate, to 103% in the cores of the large cloud entities. In addition to the low efficiency in consuming supersaturation, the high RH values in clean large clouds are due to the "protection" by large margin regions surrounding the core region.

The CvM patterns of mean margin RH show significant differences between the polluted case and the other two. The mean margin RH values of the polluted case are only marginally lower than 100%, since sub-saturated conditions within the cloud are quickly adjusted by efficient evaporation. Only the largest clouds in the polluted case permit lower mean margin RH values (~ 95%) due to the entrainment of very dry environmental pixels near the cloud tops (as seen in the vertical cross-section as well). The intermediate and clean cases show similar patterns. The smaller mass clouds (both growing and dissipating) show values above 95%, while the larger mass clouds show values as low as 85%. The larger clouds are most likely to reach low RH areas near the inversion base and below the LCL (i.e. sub-cloudy layer) and entrain dry air and by that reduce the cloud margin RH.

As seen in the vertical cross-section examples, the largest clouds in the intermediate case have even lower margin RH values than for the clean case. This can be explained by the increased development of the large intermediate clouds to heights with lower RH and by more intense downdrafts for these large clouds. The lowest RH values in the domain are seen for the precipitating fragments (i.e. located below the adiabat). These fragments typically contain low concentrations of large drop sizes (precipitation drops) which are slow to evaporate and capable of surviving in low RH conditions within the sub-cloudy layer.

Summary

In this work we explored how the aerosol effects on warm convective clouds are reflected in their partition to core and margin regions. Following part I of this work (PTI), we evaluated three types of core definitions: positive buoyancy (B_{core}), super-saturation (RH_{core}), and positive vertical velocity (W_{core}). Both single cloud and

Atmos. Chem. Phys. Discuss., https://doi.org/10.5194/acp-2018-781
Manuscript under review for journal Atmos. Chem. Phys.
Discussion started: 30 August 2018

cloud field models have been used. The former distills the dominant in-cloud processes affected by aerosols while the latter also takes into consideration the multiple temporal cloud evolution pathways and the additional effects of cloud field organization and interactions between clouds.

For all aerosol concentrations, it is shown that the self-contained property of different core types (i.e. $B_{core} \subseteq RH_{core} \subseteq W_{core}$ is maintained for clouds during their growing and mature stages. This is especially robust for the $RH_{core} \subseteq W_{core}$ subset. The W_{core} and RH_{core} volume fractions decrease monotonically during cloud growth, while B_{core} initially increases and then decreases after convection ceases. During growth, the RH_{core} (B_{core}) volume fractions are largest for clean (polluted) clouds. This is due to low (high) diffusion efficiencies, respectively, where efficient condensation promotes B_{core} at the expense of theRH_{core}.

During dissipation stages cores frequently cease to be subsets of one another and may either increase or decrease in their volume fractions. In cloud fields we also observe small cloud fragments which shed off larger cloud entities. This shedding increases for the lower concentration simulation which produce long-lived large cloud entities. These fragments show large variance in volume fraction (for all core types) magnitudes without any consistent behavior. This is due to the fact that they shed off various locations of the cloud. The polluted, non-precipitating cases, are unique in that can one expect the B_{core} to decrease monotonically and remain the smallest and a proper subset of the other cores.

For low aerosol concentration, clouds which are capable of producing precipitation, a B_{core} may form during dissipation and exist independently of the other core types. These cores are typically located at the periphery of large clouds, or throughout small precipitation or dissipating cloud fragments. The increase in B_{core} during dissipation typically coincides with precipitation production. The fluctuations in B_{core} for low concentrations may also create a subsequent W_{core}, but not of sufficient strength to also create a RH_{core}. Hence, the RH_{core} can be considered the most "well-behaved" and indicative of cloud lifetime, generally monotonically decreasing in volume fraction irrespective of aerosol concentration.

We show that the B_{core}in the warm convective cases considered here may form by two main processes:

Atmos. Chem. Phys. Discuss., https://doi.org/10.5194/acp-2018-781
Manuscript under review for journal Atmos. Chem. Phys.
Discussion started: 30 August 2018

Atmospheric Chemistry and Physics
Discussions

1. Convection: adiabatic cooling within updrafts promotes supersaturation, condensation, and release of latent heat.
2. Adiabatic heating: weak downdrafts during dissipation or precipitation transport higher potential temperatures from above.

The convective case is seen for all aerosol concentrations, and is characterized by a dependent B_{core} (i.e. $B_{core} \in RH_{core}, W_{core}$). During convection B_{core} pixels have a positive humidity term (B_{Qv}), with an increasing abundance of a positive temperature term (B_T) pixels with increase in cloud maximum vertical velocities. During dissipation this type of B_{core} shrinks rapidly due to negative B_T. The adiabatic heating case is only seen for lower aerosol concentrations, and is characterized by independent B_{core} (i.e. $B_{core} \notin RH_{core}, W_{core}$). In this case B_T is the dominant term in the cloud. The clouds with independent B_{core} experience near neutral vertical velocities for all pixels, and typically show larger cloud mean drop sizes than for the dependent type ones.

The fact that the adiabatic heating B_{core} is absent from polluted clouds highlights the importance of mean drop size and its effect on evaporation rate. The high (low) diffusion (collision coalescence) efficiencies in polluted clouds maintain a small mean drop size and efficient evaporation during entrainment. In PTI we saw that evaporation always has a strong negative effect on buoyancy. In the polluted case the convective B_{core} disappear rapidly during dissipation and cannot form in small cloud fragments even if they experience weak downdrafts. The importance of drop size is illustrated by the fact that even for lower concentrations, clouds with independent B_{core} only exist during late dissipation and precipitating stages after drop size has grown considerably.

Focusing on cores using the RH definition, a cloud's mass (volume) is dependent primarily on the processes in its core (margin). The core increases cloud mass by condensation while the margin increases the cloud's volume by mixing with the environment, or dilution. The magnitude of the effects in each region of the cloud is strongly dependent on the aerosol concentration. Increasing the aerosol concentration increases the vapor diffusion rate, minimizing both the super-saturation and sub-saturation (absolute) values in the cloud. Thus, polluted clouds are efficient in accumulating water mass but also in losing it. This competition between the core mass

Atmos. Chem. Phys. Discuss., https://doi.org/10.5194/acp-2018-781
Manuscript under review for journal Atmos. Chem. Phys.
Discussion started: 30 August 2018

gain and margin mass loss regions is what brings about the concept of an optimal aerosol concentration (Dagan et al., 2015b), and explains why more polluted clouds are not necessarily more massive.

Polluted clouds are core dominated both in terms of mass and volume, since they can hardly maintain their margins. Clean clouds are also core dominated in terms of mass, but to a lesser degree. However, expect for the initial time of cloud formation where the entire cloud is super-saturated, clean clouds tend to be margin dominated in terms of volume for most their lifetimes. Thus, despite weaker convection in the clean clouds, their large, slow evaporating margins enable their cores (and the entire cloud) to exist for longer time spans by applying a large "protecting shield" around the core.

The different diffusion efficiencies are demonstrated by observing the relative humidity (RH) values in clouds. Cleaner clouds show larger variance in RH values. During their growing stages large super-saturation in the core and sub-saturation in the margin can be seen. During their dissipation stages clouds may exist for minutes without any cloud core, with the entire cloud at sub-saturation. Polluted clouds show the opposite, with RH values nearing 100% throughout the cloud, at all stages. Hence, above a certain aerosol concentration, the saturation adjustment approximation (i.e. instant condensation of all super-saturation) can be considered valid. However, the transition from clean to polluted is not always linear. For example, for the largest clouds in the intermediate case have lower margin RH value than both the clean and polluted cases. This is due to the fact that the intermediate case manages to develop taller (than the clean case) clouds with stronger updrafts and downdrafts which entrain drier air from above the inversion layer base, but at the same time is less efficient in evaporating (than the polluted case) water and adjusting the RH to 100%.

Finally, we note that the cloud organization also changes with aerosol concentration, and thus serves as an additional factor affecting the cloud partition to core and margin. Decreasing the aerosol concentration increases the precipitation yield, which alters the sub-cloudy layer organization and promotes merging between different clouds (Seifert and Heus, 2013;Seigel, 2014;Heiblum et al., 2016a). These effects are minimal in the polluted cases. Hence, to a first approximation polluted cloud fields can be considered as a superposition of many single clouds while clean cloud fields behave very differently than a collection of single clean clouds. The continuous merging between clean clouds creates large cloud entities that evolve along relatively long times. These large precipitating entities also frequently shed small cloud fragments into the upper cloudy layer. This effect, combined with the low vapor diffusion, explains why clean clouds tend to be even more margin dominated (in terms of volume) during growth, while showing larger core fractions (especially B_{core}) during dissipation.

Acknowledgements

The research leading to these results was supported by the Ministry of Science & Technology, Israel (grant no. 3-14444).

References

Albrecht, B. A.: Aerosols, Cloud Microphysics, and Fractional Cloudiness, Science, 245, 1227-1230, 10.1126/science.245.4923.1227, 1989.

Altaratz, O., Koren, I., Remer, L. A., and Hirsch, E.: Review: Cloud invigoration by aerosols—Coupling between microphysics and dynamics, Atmospheric Research, 140–141, 38-60, 10.1016/j.atmosres.2014.01.009, 2014.

Andreae, M. O., Rosenfeld, D., Artaxo, P., Costa, A. A., Frank, G. P., Longo, K. M., and Silva-Dias, M. A.: Smoking rain clouds over the Amazon, Science, 303, 1337-1342, doi:10.1126/science.1092779, 2004.

Dagan, G., Koren, I., and Altaratz, O.: Aerosol effects on the timing of warm rain processes, Geophysical Research Letters, 42, 2015GL063839, 10.1002/2015GL063839, 2015a.

Dagan, G., Koren, I., and Altaratz, O.: Competition between core and periphery-based processes in warm convective clouds – from invigoration to suppression, Atmos. Chem. Phys., 15, 2749-2760, 10.5194/acp-15-2749-2015, 2015b.

Dagan, G., Koren, I., Altaratz, O., and Heiblum, R. H.: Aerosol effect on the evolution of the thermodynamic properties of warm convective cloud fields, Scientific Reports, 6, 38769, 10.1038/srep38769, 2016.

Dagan, G., Koren, I., Altaratz, O., and Heiblum, R. H.: Time-dependent, non-monotonic response of warm convective cloud fields to changes in aerosol loading, Atmos. Chem. Phys., 17, 7435-7444, 10.5194/acp-17-7435-2017, 2017.

Dey, S., Di Girolamo, L., Zhao, G., Jones, A. L., and McFarquhar, G. M.: Satellite-observed relationships between aerosol and trade-wind cumulus cloud properties over the Indian Ocean, Geophysical Research Letters, 38, L01804, 10.1029/2010GL045588, 2011.

Heiblum, R. H., Altaratz, O., Koren, I., Feingold, G., Kostinski, A. B., Khain, A. P., Ovchinnikov, M., Fredj, E., Dagan, G., Pinto, L., Yaish, R., and Chen, Q.: Characterization of cumulus cloud fields using trajectories in the center of gravity versus water mass phase space: 2. Aerosol effects on warm convective clouds, Journal of Geophysical Research: Atmospheres, 121, 6356-6373, 10.1002/2015JD024193, 2016a.

Heiblum, R. H., Altaratz, O., Koren, I., Feingold, G., Kostinski, A. B., Khain, A. P., Ovchinnikov, M., Fredj, E., Dagan, G., Pinto, L., Yaish, R., and Chen, Q.: Characterization of cumulus cloud fields using trajectories in the center of gravity versus water mass phase space: 1. Cloud tracking and phase space description, Journal of Geophysical Research: Atmospheres, 121, 6336-6355, 10.1002/2015JD024186, 2016b.

Hudson, J. G., and Yum, S. S.: Maritime–Continental Drizzle Contrasts in Small Cumuli, J Atmos Sci, 58, 915-926, 10.1175/1520-0469(2001)058<0915:mcdcis>2.0.co;2, 2001.

Hudson, J. G., and Mishra, S.: Relationships between CCN and cloud microphysics variations in clean maritime air, Geophysical Research Letters, 34, doi:10.1029/2007GL030044, 2007.

IPCC: Clouds and Aerosols, in: *Climate Change 2013 - The Physical Science Basis*, Cambridge University Press, 571-658, 2013.

Jiang, H., and Feingold, G.: Effect of aerosol on warm convective clouds: Aerosol-cloud-surface flux feedbacks in a new coupled large eddy model, J Geophys Res-Atmos, 111, 10.1029/2005jd006138, 2006.

Jiang, H., Xue, H. W., Teller, A., Feingold, G., and Levin, Z.: Aerosol effects on the lifetime of shallow cumulus, Geophysical Research Letters, 33, 10.1029/2006gl026024, 2006.

Jiang, H., Feingold, G., and Koren, I.: Effect of aerosol on trade cumulus cloud morphology, Journal of Geophysical Research: Atmospheres, 114, D11209, 10.1029/2009JD011750, 2009.

Kaufman, Y. J., Koren, I., Remer, L. A., Rosenfeld, D., and Rudich, Y.: The effect of smoke, dust, and pollution aerosol on shallow cloud development over the Atlantic

Ocean, Proceedings of the National Academy of Sciences of the United States of America, 102, 11207-11212, 10.1073/pnas.0505191102, 2005.

Khain, A. P., Pokrovsky, A., Pinsky, M., Seifert, A., and Phillips, V.: Simulation of Effects of Atmospheric Aerosols on Deep Turbulent Convective Clouds Using a Spectral Microphysics Mixed-Phase Cumulus Cloud Model. Part I: Model Description and Possible Applications, J Atmos Sci, 61, 2963-2982, 10.1175/JAS-3350.1, 2004.

Khain, A. P., Rosenfeld, D., and Pokrovsky, A.: Aerosol impact on the dynamics and microphysics of deep convective clouds, Quarterly Journal of the Royal Meteorological Society, 131, 2639-2663, 10.1256/qj.04.62, 2005.

Khairoutdinov, M. F., and Randall, D. A.: Cloud Resolving Modeling of the ARM Summer 1997 IOP: Model Formulation, Results, Uncertainties, and Sensitivities, J Atmos Sci, 60, 607-625, 10.1175/1520-0469(2003)060<0607:CRMOTA>2.0.CO;2, 2003.

Kogan, Y. L., and Martin, W. J.: Parameterization of Bulk Condensation in Numerical Cloud Models, J Atmos Sci, 51, 1728-1739, 10.1175/1520-0469(1994)051<1728:POBCIN>2.0.CO;2, 1994.

Köhler, H.: The nucleus in and the growth of hygroscopic droplets, Transactions of the Faraday Society, 32, 1152-1161, 1936.

Koren, I., Dagan, G., and Altaratz, O.: From aerosol-limited to invigoration of warm convective clouds, Science, 344, 1143-1146, 10.1126/science.1252595, 2014.

Koren, I., Altaratz, O., and Dagan, G.: Aerosol effect on the mobility of cloud droplets, Environmental Research Letters, 10, 104011, 10.1088/1748-9326/10/10/104011, 2015.

L'Ecuyer, T. S., Berg, W., Haynes, J., Lebsock, M., and Takemura, T.: Global observations of aerosol impacts on precipitation occurrence in warm maritime clouds, Journal of Geophysical Research: Atmospheres, 114, doi:10.1029/2008JD011273, 2009.

Li, Z., Niu, F., Fan, J., Liu, Y., Rosenfeld, D., and Ding, Y.: Long-term impacts of aerosols on the vertical development of clouds and precipitation, Nature Geoscience, 4, 888-894, 10.1038/ngeo1313, 2011.

Mason, B., and Chien, C.: Cloud-droplet growth by condensation in cumulus, Quarterly Journal of the Royal Meteorological Society, 88, 136-142, 1962.

Atmos. Chem. Phys. Discuss., https://doi.org/10.5194/acp-2018-781
Manuscript under review for journal Atmos. Chem. Phys.
Discussion started: 30 August 2018

Mordy, W.: Computations of the growth by condensation of a population of cloud droplets, Tellus, 11, 16-44, 10.1111/j.2153-3490.1959.tb00003.x, 1959.

Pinsky, M., Mazin, I. P., Korolev, A., and Khain, A. P.: Supersaturation and Diffusional Droplet Growth in Liquid Clouds, J Atmos Sci, 70, 2778-2793, 10.1175/JAS-D-12-077.1, 2012.

Reisin, T., Levin, Z., and Tzivion, S.: Rain Production in Convective Clouds As Simulated in an Axisymmetric Model with Detailed Microphysics. Part I: Description of the Model, J Atmos Sci, 53, 497-519, 10.1175/1520-0469(1996)053<0497:RPICCA>2.0.CO;2, 1996.

Reutter, P., Su, H., Trentmann, J., Simmel, M., Rose, D., Gunthe, S. S., Wernli, H., Andreae, M. O., and Pöschl, U.: Aerosol-and updraft-limited regimes of cloud droplet formation: influence of particle number, size and hygroscopicity on the activation of cloud condensation nuclei (CCN), Atmos Chem Phys, 9, 7067-7080, 10.5194/acp-9-7067-2009, 2009.

Savane, O., Vant-Hull, B., Mahani, S., and Khanbilvardi, R.: Effects of Aerosol on Cloud Liquid Water Path: Statistical Method a Potential Source for Divergence in Past Observation Based Correlative Studies, Atmosphere, 6, 273, 10.3390/atmos6030273, 2015.

Seifert, A., and Heus, T.: Large-eddy simulation of organized precipitating trade wind cumulus clouds, Atmos. Chem. Phys., 13, 5631-5645, 10.5194/acp-13-5631-2013, 2013.

Seifert, A., Heus, T., Pincus, R., and Stevens, B.: Large-eddy simulation of the transient and near-equilibrium behavior of precipitating shallow convection, J Adv Model Earth Sy, 7, 1918-1937, 10.1002/2015MS000489, 2015.

Seigel, R. B.: Shallow Cumulus Mixing and Subcloud-Layer Responses to Variations in Aerosol Loading, J Atmos Sci, 71, 2581-2603, 10.1175/JAS-D-13-0352.1, 2014.

Seiki, T., and Nakajima, T.: Aerosol Effects of the Condensation Process on a Convective Cloud Simulation, J Atmos Sci, 71, 833-853, 10.1175/JAS-D-12-0195.1, 2013.

Siebesma, A. P., Bretherton, C. S., Brown, A., Chlond, A., Cuxart, J., Duynkerke, P. G., Jiang, H., Khairoutdinov, M. F., Lewellen, D., and Moeng, C. H.: A large eddy simulation intercomparison study of shallow cumulus convection, J Atmos Sci, 60, 1201-1219, 10.1175/1520-0469(2003)60<1201:ALESIS>2.0.CO;2, 2003.

Atmos. Chem. Phys. Discuss., https://doi.org/10.5194/acp-2018-781
Manuscript under review for journal Atmos. Chem. Phys.
Discussion started: 30 August 2018

Small, J. D., Chuang, P. Y., Feingold, G., and Jiang, H.: Can aerosol decrease cloud lifetime?, Geophysical Research Letters, 36, n/a-n/a, 10.1029/2009GL038888, 2009.

Sorooshian, A., Feingold, G., Lebsock, M. D., Jiang, H., and Stephens, G. L.: On the precipitation susceptibility of clouds to aerosol perturbations, Geophysical Research Letters, 36, L13803, 10.1029/2009GL038993 2009.

Squires, P.: The Microstructure and Colloidal Stability of Warm Clouds, Tellus, 10, 256-261, 10.1111/j.2153-3490.1958.tb02011.x, 1958.

Stevens, B.: On the Growth of Layers of Nonprecipitating Cumulus Convection, J Atmos Sci, 64, 2916-2931, 10.1175/JAS3983.1, 2007.

Stevens, B., and Feingold, G.: Untangling aerosol effects on clouds and precipitation in a buffered system, Nature, 461, 607-613, 10.1038/nature08281, 2009.

Twomey, S.: The influence of pollution on the shortwave albedo of clouds, J Atmos Sci, 34, 1149-1152, 10.1175/1520-0469(1977)034<1149:TIOPOT>2.0.CO;2, 1977.

Tzivion, S., Feingold, G., and Levin, Z.: An efficient numerical solution to the stochastic collection equation, J Atmos Sci, 44, 3139-3149, 10.1175/1520-0469(1987)044<3139:AENSTT>2.0.CO;2, 1987.

Wang, C.: A modeling study of the response of tropical deep convection to the increase of cloud condensation nuclei concentration: 1. Dynamics and microphysics, Journal of Geophysical Research: Atmospheres, 110, D21211, 10.1029/2004JD005720, 2005.

Warner, J.: A Reduction in Rainfall Associated with Smoke from Sugar-Cane Fires—An Inadvertent Weather Modification?, Journal of Applied Meteorology, 7, 247-251, 10.1175/1520-0450(1968)007<0247:ARIRAW>2.0.CO;2, 1968.

Xue, H. W., and Feingold, G.: Large-eddy simulations of trade wind cumuli: Investigation of aerosol indirect effects, J Atmos Sci, 63, 1605-1622, 10.1175/jas3706.1, 2006.

Xue, H. W., Feingold, G., and Stevens, B.: Aerosol effects on clouds, precipitation, and the organization of shallow cumulus convection, J Atmos Sci, 65, 392-406, 10.1175/2007jas2428.1, 2008.

Yuan, T., Remer, L. A., and Yu, H.: Microphysical, macrophysical and radiative signatures of volcanic aerosols in trade wind cumulus observed by the A-Train, Atmos. Chem. Phys., 11, 7119-7132, 10.5194/acp-11-7119-2011, 2011.

Atmos. Chem. Phys. Discuss., https://doi.org/10.5194/acp-2018-781
Manuscript under review for journal Atmos. Chem. Phys.
Discussion started: 30 August 2018

Atmospheric Chemistry and Physics
Discussions

Figures

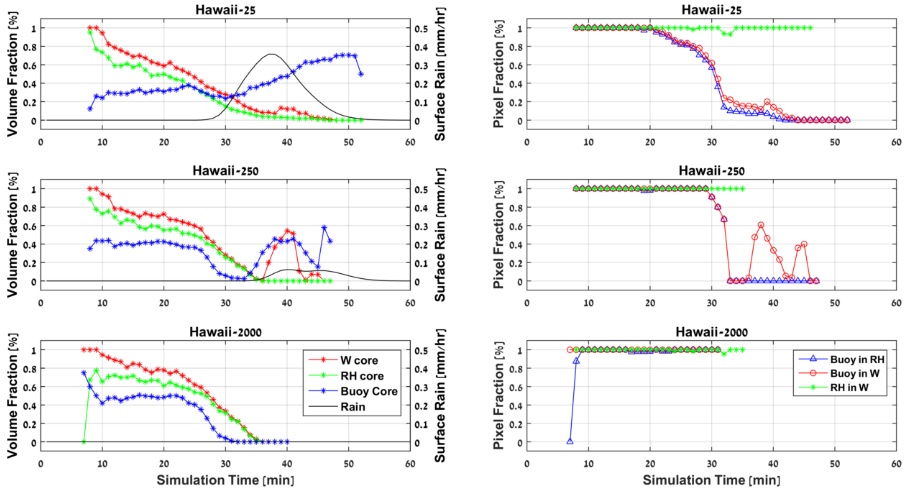

Figure 1. Left: Time series of core volume fractions ([%], LHS axis) and surface rain-rate ([mm hr^{-1}], RHS axis) for the clean (top panel), intermediate (middle panel), and polluted (bottom panel) single cloud simulations. Right: Time series of core pixel fractions within other core types [%], for the respective simulation types. Core volume and pixel fractions are indicated by different line colors (see legends).

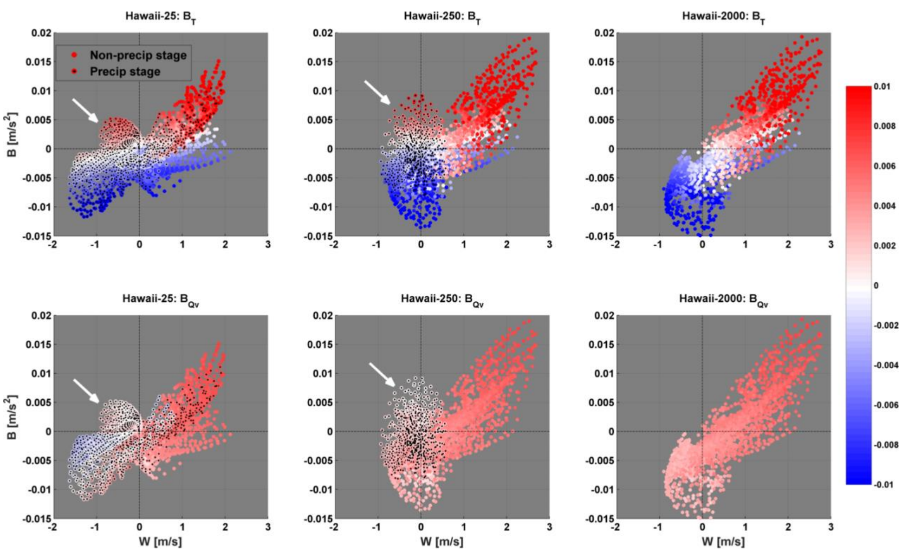

Figure 2. Scatter plots of pixel total buoyancy [m s^{-2}] vs. pixel vertical velocity [m s^{-1}], for the clean (left), intermediate (middle), and polluted (right) simulations. Data includes all cloudy pixels during all time steps. Colors represent magnitude of buoyancy temperature term (B_T, upper row) and humidity term (B_{Qv}, lower row), where red (blue) shades indicate positive (negative) values. Markers with black dots superimposed represent temporal stages with non-zero surface precipitation. White arrows indicate outlier scatter of pixels with positive buoyancy and negative vertical velocity.

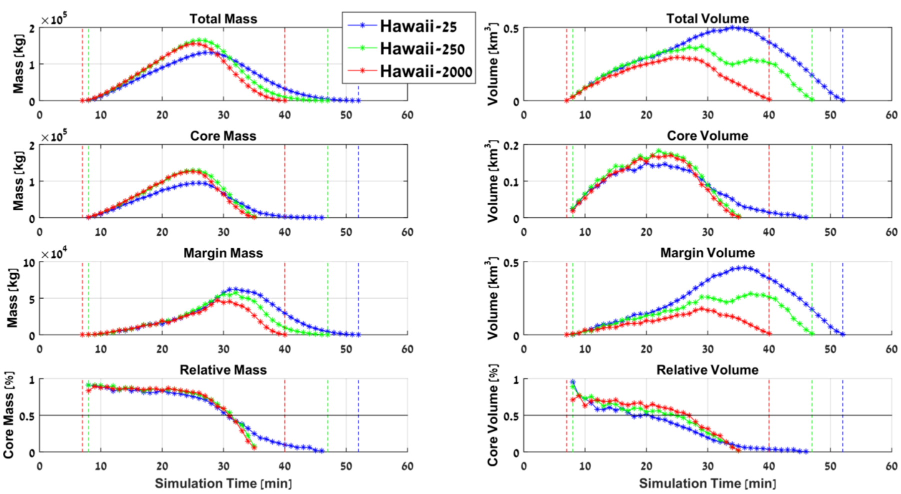

Figure 3. Time series of cloud mass ([kg], left column) and cloud volume ([km^3], right column) for the different aerosol concentrations simulations (see legend). The total, core, margin, and relative fraction values are shown for each parameter, as indicated by panel titles. The core here is defined according to RH>100% definition.

Atmos. Chem. Phys. Discuss., https://doi.org/10.5194/acp-2018-781
Manuscript under review for journal Atmos. Chem. Phys.
Discussion started: 30 August 2018

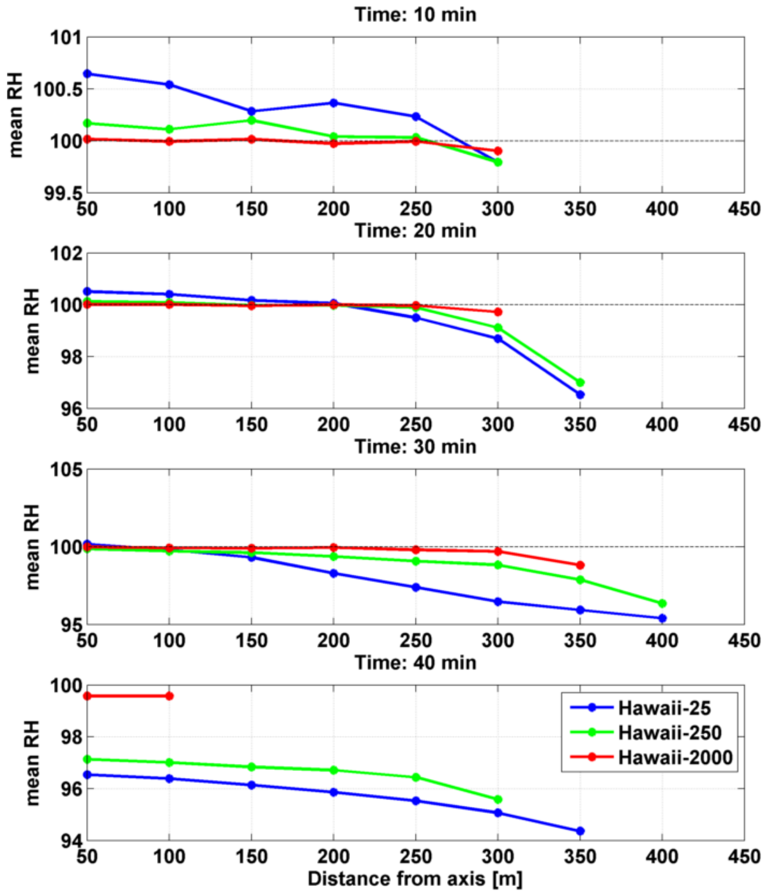

Figure 4. Four temporal snapshots (see panel titles for times) of RH [%] horizontal cross-sections. Panels include the results of different aerosol concentrations (see legend). Cross-sections are obtained by taking the mean RH of all vertical levels for each horizontal distance from the cloud center axis.

Atmos. Chem. Phys. Discuss., https://doi.org/10.5194/acp-2018-781
Manuscript under review for journal Atmos. Chem. Phys.
Discussion started: 30 August 2018

Atmospheric Chemistry and Physics
Open Access
Discussions

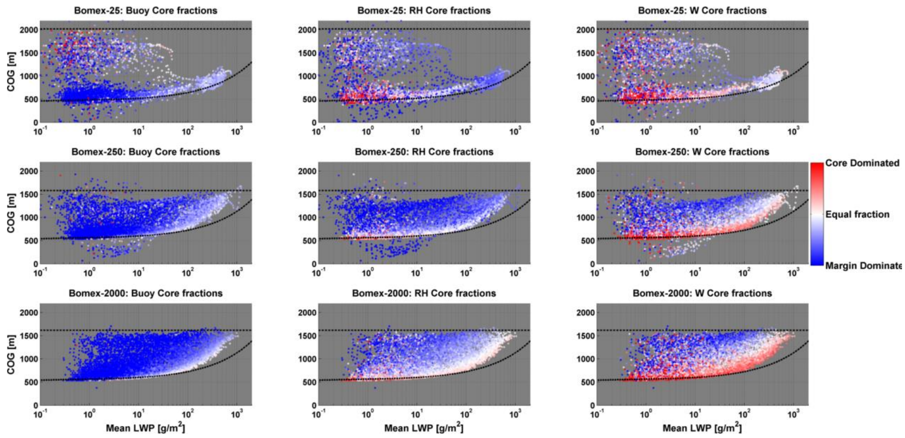

Figure 5. CvM phase space diagrams of B_{core} (left column), RH_{core} (middle column), and W_{core} (right column) volume fractions for all clouds between 3 h and 8 h in the BOMEX simulations. The upper, middle, and lower panels correspond to the clean, intermediate, and polluted aerosol cases. The red (blue) colors indicate a core volume fraction above (below) 0.5. The majority of clouds are confined to the region between the adiabatic cloud growth approximation (curved dashed line) and the inversion layer base height (horizontal dashed line). For an in-depth description of CvM space characteristics, the reader is referred to Sect. 2.4 in PTI.

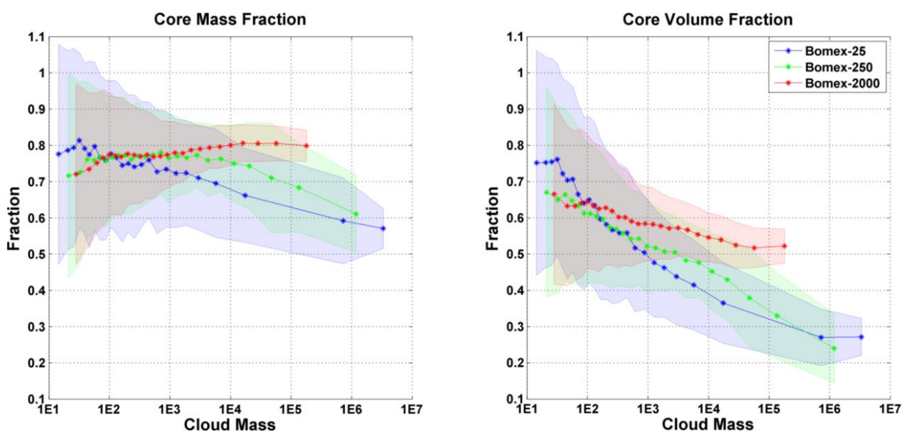

Figure 6. Average core mass fraction (left) and volume fraction (right) values for different aerosol concentrations, as indicated in the legend. The average only includes

Atmos. Chem. Phys. Discuss., https://doi.org/10.5194/acp-2018-781
Manuscript under review for journal Atmos. Chem. Phys.
Discussion started: 30 August 2018

growing branch clouds from within the CvM space (i.e. clouds located in proximity to the adiabat). The core here is defined according to RH>100% definition.

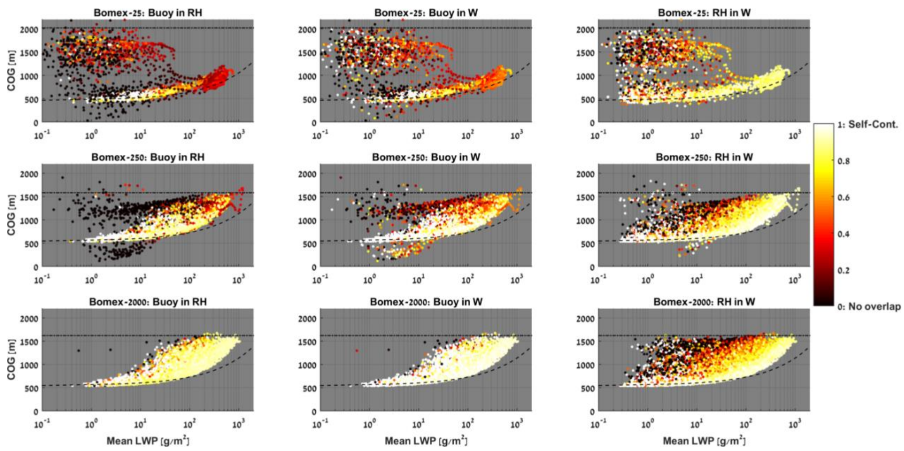

Figure 7. CvM space diagrams showing the pixel fractions of B_{core} within RH_{core}, W_{core}, and RH_{core} within W_{core} (as indicated in the panel titles). Bright colors indicate high pixel fractions (large overlap between two core types) while dark colors indicate low pixel fraction (little overlap between two core types). The differences in the scatter density and location for different panels are due to the fact that only clouds which contain a core fraction above zero (for the core in question) are considered.

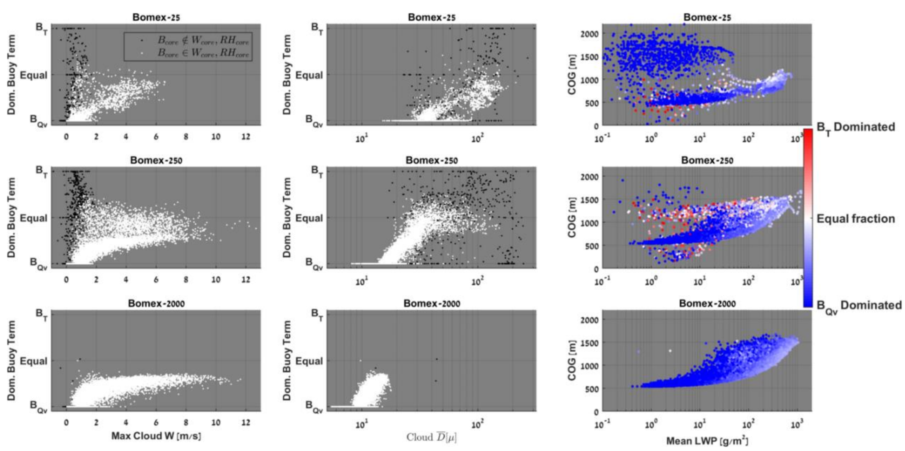

Atmos. Chem. Phys. Discuss., https://doi.org/10.5194/acp-2018-781
Manuscript under review for journal Atmos. Chem. Phys.
Discussion started: 30 August 2018

Figure 8. Analysis of dominant buoyancy term within B_{core} of clouds (see text for details). As seen in previous figures, rows represent clean (top), intermediate (middle), and polluted (bottom) simulations. Left: dependence on maximum vertical velocity within cloud. Middle: dependence on partition of total cloud mass to cloud droplets and rain drops. Right: CvM space diagrams of all clouds with B_{core}, where red (blue) shades indicate temperature (humidity) buoyancy terms dominate the cloud.

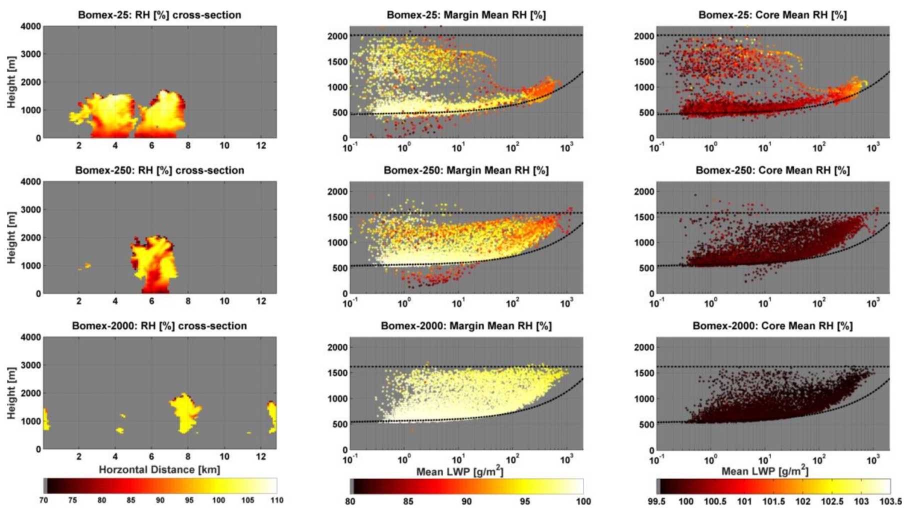

Figure 9. Left column – Relative Humidity (RH [%]) vertical cross-sections slicing through the center of gravity of the most massive cloud in each simulation. Middle and right columns display CvM space diagrams of mean cloud margin RH and mean cloud core RH, respectively, using the RH_{core} definition. The upper, middle, and lower panels correspond to the clean, intermediate, and polluted aerosol cases (see panel titles). Notice the different color bar ranges for margin and core mean RH panels.